21st European Symposium on Computer Aided Process Engineering – ESCAPE 21
E.N. Pistikopoulos, M.C. Georgiadis and A.C. Kokossis (Editors)

Predicting microbial growth kinetics with the use of genetic circuit models

Michalis Koutinas,[a] Alexandros Kiparissides,[a] Victor de Lorenzo,[b] Vitor A.P. Martins dos Santos,[c] Efstratios N. Pistikopoulos,[a] Athanasios Mantalaris[a]

[a]*Department of Chemical Engineering and Chemical Technology, Imperial College London, SW7 2AZ, London, United Kingdom*

[b]*Centro Nacional de Biotecnologia, Consejo Superior de Investigaciones Cientificas, Darwin 3, Cantoblanco, 28049 Madrid, Spain*

[c]*Chair for Systems and Synthetic Biology, Wageningen University, Dreijenplein 310, 6703 HB Wageningen, The Netherlands*

Abstract

A novel modeling approach for the description of bioprocesses is proposed, linking microbial growth kinetics to gene regulation. An example is given with the development and experimental validation of a dynamic mathematical model of the TOL plasmid of *Pseudomonas putida* mt-2, which is used for the metabolism of *m*-xylene. The model of this genetic circuit is coupled to a growth kinetic model through predictions of rate-limiting enzyme concentrations that control biomass growth and substrate consumption. Batch cultures of mt-2 fed with *m*-xylene were performed to estimate model parameters and to confirm that the combined model successfully describes the bioprocess, through mRNA, biomass and *m*-xylene concentration measurements. However, mathematical models developed exclusively based on macroscopic measurements failed to predict the process variables, highlighting the importance of gene regulation for the development of advanced biological models.

Keywords: Dynamic modeling, Genetic circuit, pWW0 (TOL) plasmid; *m*-xylene.

1. Introduction

Monitoring of bioprocess performance is often conducted based on bulk measurements ignoring regulation at the genetic level [1]. Although modern molecular tools, such as RT-PCR, have been previously applied to improve the monitoring of in situ microbial function, substrate consumption is usually correlated to mRNA levels using best-fit lines ignoring the regulatory loops controlling the transcription from catabolic genes [2]. Therefore, the relationship between mRNA concentration and cellular activity can be dependent on the experimental conditions, highlighting the need for establishing mechanistic models that link gene transcript levels and substrate consumption rates.

Pseudomonas putida is a metabolically versatile bacterium exhibiting a wide biotechnological potential. Strain *P. putida* mt-2 is equipped with the TOL plasmid (pWW0), which specifies a pathway for the catabolism of major environmental pollutants, such as *m*-xylene. The required genetic machinery for the metabolism of *m*-xylene is encoded by the *upper* and *meta* gene operons of the plasmid, which synthesize the required enzymes for the conversion of *m*-xylene to Krebs cycle intermediates, while *xylS* and *xylR* are involved in transcriptional control [3].

This work presents the construction of a dynamic model relevant to the function of *Pu* and *Pm* promoters of TOL, controlling the transcription from its catabolic operons. Computation of the rate-limiting enzymes synthesized by the operons is linked to specific growth and substrate utilization rates demonstrating that the combined model successfully describes the dynamics of the system. The prediction of the combined model is compared to that of Monod-type models underlying the importance of this novel modeling approach for improving the prediction of microbial growth kinetics.

2. Results and discussion

2.1. Genetic circuit model

We have recently developed a dynamic mathematical model describing the function of *Ps/Pr* promoters of TOL, involved in the transcriptional control of the plasmid's operons, as well as the production of $XylR_i$ and its subsequent multimerization to $XylR_a$ [4]. Therefore, this part of the TOL model is not presented here and can be obtained from the reference given above. In the present work, we extend this model to include predictions of *Pu* and *Pm* promoters driven transcription leading to the synthesis of the enzymes of the pathway. The TOL network has been reconstructed into its various molecular elements and has been described as a combination of logic gates (Figure 1). Therefore, based on this logic model Hill functions were used as input functions to the genes producing a dynamic mathematic model, which is presented below.

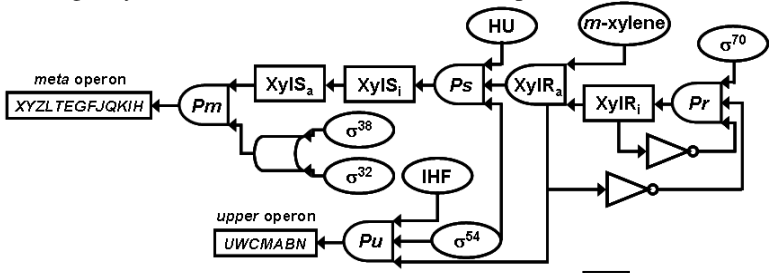

Figure 1. Logic model of the TOL (pWW0) plasmid. ⬭ : input; ▭ : output; ⊂ : AND; ⋃ : OR; ▷ : NOT.

Transcription from the *upper* pathway is driven by the *Pu* promoter, which is triggered by the activated form of XylR protein ($XylR_a$). The binding of $XylR_a$ to the promoter and the looping out of the complex closely to the σ^{54}-RNAp complex is assisted by the integration host factor (IHF), stimulating the production of the *upper* operon enzymes. We have assumed that the concentrations of σ^{54} and IHF are constant at housekeeping

level. Thus, the function of the relative mRNA concentration of *Pu* is given by Eq. (1) (equations are given in Table 1 and symbols are defined in Table 2).

Table 1. Model equations.

Equations	Number	Equations	Number
$\frac{dPu_{TC}}{dt} = \beta_{Pu} \frac{XylR_a}{K_{XylR_a,Pu} + XylR_a} - \alpha_{Pu} Pu_{TC}$	(1)	$\mu = \frac{\beta_{XylM,b} XylM}{K_{XylM,b} + XylM}$	(8)
$\frac{dXylU}{dt} = \beta_{XylU} Pu_{TC} - \alpha_{XylU} XylU$	(2)	$\frac{dX}{dt} = (\mu - d)X$	(9)
$\frac{dXylS_i}{dt} = \beta_{XylS_i} Ps_{TC} - r_{XylS} XylS_i + 2r_{R,XylS} XylS_a - \alpha_{XylS_i} XylS_i$	(3)	$d = \frac{d_{\max} Xyl}{K_d + Xyl}$	(10)
$\frac{dXylS_a}{dt} = \frac{1}{2} r_{XylS} XylS_i - r_{R,XylS} XylS_a$	(4)	$\mu = \frac{\mu_{\max,1} Xyl}{K_{S,1} + Xyl}$	(11)
$\frac{dPm_{TC}}{dt} = \beta_{Pm} \frac{XylS_a}{K_{XylS_i,Pm} + XylS_a} \frac{XylS_i^2}{K_{XylS_i,Pm}^2 + XylS_i^2} - \alpha_{Pm} Pm_{TC}$	(5)	$\mu = \frac{\mu_{\max,2} Xyl}{K_{S,2} + Xyl + \frac{Xyl^3}{K_I^2}}$	(12)
$\frac{dXylM}{dt} = \beta_{XylM} Pm_{TC} - \alpha_{XylM} XylM$	(6)	$\frac{dXyl}{dt} = -\frac{\mu}{Y} X$	(13)
$\frac{dXyl}{dt} = -\frac{1}{MW_{m-x}} \frac{\beta_{XylU,m-x} XylU}{K_{XylU,m-x} + XylU} X$	(7)		

Table 2. List of symbols.

Symbols	Definition
d / d_{max}	decay and maximum decay rates
K_d / $K_{S,1}$ / $K_{S,2}$	decay and *m*-xylene saturation constants
K_I	*m*-xylene inhibition constant
$K_{XylM,b}$	saturation constant for XylM
$K_{XylRa,Pu}$ / $K_{XylSi,Pm}$	activation coefficients of *Pu* and *Pm* due to $XylR_a$ and $XylS_i$
MW_{m-x}	*m*-xylene molecular weight
Pu_{TC} / Pm_{TC} / Ps_{TC}	relative mRNA concentrations of *Pu*, *Pm* and *Ps*
r_{XylS} / $r_{R,XylS}$	$XylS_i$ oligomerization and $XylS_a$ dissociation constants
t	time
Xyl / X	*m*-xylene and biomass concentrations respectively
$XylR_i$ / $XylR_a$ / $XylS_i$ / $XylS_a$	concentrations of the inactive and active forms of XylR and XylS proteins
XylU / XylM	concentrations of the rate-limiting enzymes of the *upper* and *meta* pathways
Y	yield coefficient for biomass on *m*-xylene
α_{Pu} / α_{Pm}	mRNA degradation rates of *Pu* and *Pm*
α_{XylU} / α_{XylM} / α_{XylSi}	XylU, XylM and $XylS_i$ degradation/dilution rates due to cellular volume increase
β_{Pu} / β_{Pm}	maximal expression levels of *Pu* and *Pm*
$\beta_{XylM,b}$	maximum specific growth rate of biomass based on XylM
β_{XylU} / β_{XylM} / β_{XylSi}	translation rates based of *Pu*, *Pm* and *Ps* mRNA
$\beta_{XylU,m-x}$	maximum *m*-xylene metabolic quotient based on XylU
μ / $\mu_{max,1}$ / $\mu_{max,2}$	specific and maximum specific growth rates of biomass on *m*-xylene

The enzymatic products of the *upper* operon oxidize *m*-xylene to 3-methylbenzoate in a series of reactions. Moreover, although the control of the enzyme level on the flux of a pathway is distributed between all participating enzymes, these enzymes do not always

exert the same level of control on the flux, which is usually dominated by a single rate-limiting enzyme [5]. Due to the fact that the production of the rate-limiting enzyme required for the reactions of the *upper* pathway is controlled by *Pu*, this production is expressed as a function of the relative mRNA concentration of the promoter (Eq. 2).
The *xylS* gene is transcribed by the σ^{54}-dependent *Ps* promoter synthesizing the XylS protein. In the presence of *m*-xylene, the high XylS concentration produced leads to dimerization of XylS monomers stimulating transcription from *Pm*. Eqs. (3,4) describe the production of XylS from *Ps* driven transcription and XylS activation/deactivation.
The *Pm* promoter controls transcription from the *meta* operon triggered by the activated form of XylS ($XylS_a$) and σ^{32} or σ^{38} depending on the growth phase. Since the $XylS_i$ monomer also binds to *Pm*, the relative mRNA concentration of *Pm* is expressed by Eq. (5). Similarly to the assumption made for the *upper* pathway, the conversion of 3-methylbenzoate to Krebs cycle intermediates in the *meta* pathway is modeled as being exclusively controlled by a single rate-limiting enzyme. Thus, the synthesis of this enzyme is expressed as a function of the relative mRNA concentration of *Pm* (Eq. 6).

2.2. Linking the genetic circuit model to the growth kinetics

A model linking the mRNA transcript levels predicted by the TOL model to the growth kinetics of mt-2 has been developed. The *upper* pathway drives the first reaction for *m*-xylene bioconversion to TOL pathway intermediates, while the *meta* pathway channels the metabolic products of TOL into the Krebs cycle resulting in biomass growth. Thus, *m*-xylene consumption is given as a function of the concentration of the rate-limiting enzyme controlled by *Pu* (Eq. 7) and the specific growth rate on *m*-xylene is expressed as a function of the concentration of the rate-limiting enzyme controlled by *Pm* (Eq. 8). Biomass production and decay are modelled using Eqs. (9,10).
In many cases the Monod equation is used to model the specific growth rate (Eq. 11). Also, when an inhibitory substrate such as *m*-xylene is fed, the Yano and Koga model [6] accounting for substrate inhibition can be used (Eq. 12). Therefore, the consumption of the substrate is given by Eq. (13) and biomass production is expressed by Eq. (9).

2.3. Predicting the growth kinetics with the combined model

The parameters of the combined, Monod and Yano and Koga models were obtained in a batch experiment where mt-2 was grown with 1 mM *m*-xylene (data not shown). Thus, the predictive capability of these models was tested in a batch culture fed with 0.4 mM *m*-xylene. The overall trend of the model's prediction for *Pu* and *Pm* was accurate (Figs. 2A,B), confirming that its structure successfully describes the experiment.
Based on the TOL model, the concentrations of the rate-limiting enzymes of the two pathways were calculated for this experiment (Figs. 2C,D). According to the measured biomass and *m*-xylene concentrations, the duration of the lag-phase was 10 min. Thus, for the observed duration of the lag-phase we have fitted the three models developed to the average values of the experimental points. However, since the response of TOL starts immediately following introduction of the substrate, the TOL model was simulated from the beginning of the experiment. The Monod, and Yano and Koga models failed to predict this experiment, calculating significantly higher biomass production compared to that measured experimentally (Figs. 2E,F). On the other hand,

the combined model accurately described the experiment demonstrating the importance of considering the regulatory effects of a key circuit for predicting the bioprocess.

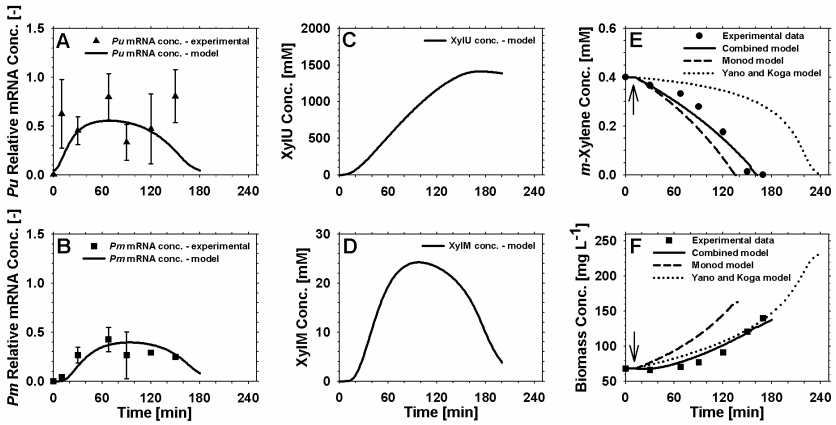

Figures 2A-F. Comparison of the three models developed in the predictive experiment. The arrows indicate the duration of the lag-phase.

3. Conclusions

We have built and validated a dynamic mathematical model that accounts for the regulatory features of the TOL plasmid. The function of TOL has been linked to the growth kinetics of mt-2 developing a systematic framework that couples gene expression to macroscopic bioprocess behaviour. This work demonstrates that substrate consumption and biomass production can be decoupled and described in a mechanistic way based on the molecular interactions regulating the two processes, while the presence of non-constant yields can be also considered. Thus, the accuracy of models in the field can be improved with quantitative descriptions of the regulatory effects controlling upstream the production of catabolic enzymes.

4. Acknowledgements

The following EU projects have supported this work: a) PROBACTYS (EU – FP6), b) PSYSMO (BBSRC – ERA-NET program) and c) TARPOL (EU – FP7).

References

[1] J.B. Rogers, K.F. Reardon, (2000) Biotechnol. Bioeng. 70, 428
[2] J.E. Corredor, B. Wawrik, J.H. Paul, H. Tran, L. Kerkhof, et al., (2004) Appl. Environ. Microbiol. 70, 5459
[3] J.L. Ramos, S. Marques, K.N. Timmis, (1997) Annu. Rev. Microbiol. 51, 341
[4] M. Koutinas, M.-C. Lam, A. Kiparissides, R. Silva-Rocha, M. Godinho, et al., (2010) Environ. Microbiol. 12, 1705
[5] R.D. Douma, P.J.T. Verheijen, W.T.A.M. de Laat, J.J. Heijnen, W.M. van Gulik, (2010) Biotechnol. Bioeng. 106, 608
[6] T. Yano, S. Koga, (1969) Biotechnol. Bioeng. 11, 139